ELSEVIER

Energy Conversion and Management 45 (2004) 865–881

ENERGY CONVERSION & MANAGEMENT

www.elsevier.com/locate/enconman

Sequential design of decentralized load frequency controllers using μ synthesis and analysis

H. Bevrani *, Y. Mitani, K. Tsuji

Department of Electrical Engineering, Osaka University, 2-1 Yamada-Oka, Suita, Osaka 565-0871, Japan

Received 5 March 2003; accepted 16 July 2003

Abstract

A new systematic approach to design of sequential decentralized load frequency controllers for multi-area power systems based on μ synthesis and analysis is described. System uncertainties, practical constraints on control action and desired performance are included in the synthesis procedure. The robust performance in terms of the structured singular value is used as a measure of control performance. A four area power system example is presented, demonstrating the controllers' synthesis procedure and advantages of the proposed strategy.

Keywords: Load frequency control; Decentralized control; Sequential design; μ synthesis

1. Introduction

The load frequency control (LFC) problem has been one of the major subjects in electric power system design/operation and is becoming much more significant today in accordance with the increasing size and complexity of interconnected power systems. There has been continuing interest in designing load frequency controllers with better performance to maintain the frequency and to keep tie line power flows within pre-specified values, using various decentralized control methods during the last two decades [1–10].

Simultaneous design for a fixed controller structure is used in all reported decentralized LFC scenarios, which is difficult numerically for large scale power systems, and it does not provide some of the advantages that are usually the reason for using decentralized control in the first place, such

* Corresponding author. Tel.: +81-6-6879-7712; fax: +81-6-6879-7713.
E-mail address: bevrani@polux.pwr.eng.osaka-u.ac.jp (H. Bevrani).

0196-8904/$ - see front matter © 2003 Elsevier Ltd. All rights reserved.
doi:10.1016/S0196-8904(03)00196-1

as the ability to bring the system into service by closing one loop at a time and the guarantee of stability and performance in the case of failures. In addition, some proposed methods might not work properly and do not guarantee performance when the operating points vary.

In this paper, a new systematic approach to sequential decentralized LFC design in a multi-area power system based on structured singular value theory (μ) is described. The sequential control design, because of its advantages, is the most common design procedure in real applications of decentralised synthesis methods. Sequential design involves closing and tuning one loop at a time. This method is less conservative than independent decentralised design because, at each design step one utilizes the information about the controller specified in the previous step [11], and also, it is more practical in comparison with common decentralized methods.

After introducing the μ based sequential control framework and pairing inputs and outputs, we will design a single input single output (SISO) controller for each loop (control area). In load frequency controller design for each area, the structured singular value, introduced by Doyel et al. [12] will be used as a synthesis tool and a measure of performance robustness. This paper shows μ synthesis can be successfully used for sequential design of multi-area power system load frequency controllers that guarantee robust stability and robust performance for a wide range of operating conditions. The preliminary step of this work is presented in Ref. [13].

This paper is organized as follows. Section 2 describes the control area model. Synthesis methodology is given in Section 3. In Section 4, the proposed strategy is applied to a four area power system, and finally some simulation results are given in Section 5 to demonstrate the effectiveness of the proposed scheme.

2. Model description

In this paper, we use the conventional model for each control area of a multi-area power system, which is widely used by researchers [1–10]. Actually, power systems have a highly non-linear and time varying nature. However, a simplified and linearized model is usually used for LFC. The error caused by the simplification and linearization can be considered in robust control strategies (such as μ synthesis).

In each control area, we have considered three simple transfer functions according to the generator, turbine and power system (rotating mass and load). Fig. 1 shows the block diagram of control area-1 from an n-area power system. The connections of area-1 to other areas are shown in this figure. Referring to Fig. 1, the state space realization of area i is given by

$$\begin{aligned} \dot{x}_i &= A_i x_i + B_i u_i + F_i d_i \\ y_i &= C_i x_i \end{aligned} \tag{1}$$

The state vector x_i, control input u_i and disturbance input d_i can be defined as follows:

$$x_i = [\, \Delta f_i \quad \Delta P_{ti} \quad \Delta P_{gi} \quad \Delta P_{tie-i} \,]^{\mathrm{T}}, \quad u_i = \Delta P_{ci}, \quad d_i = \Delta P_{di} \tag{2}$$

where

Δf_i incremental frequency deviation of area-i
ΔP_{gi} incremental governor valve position change of generator in area-i

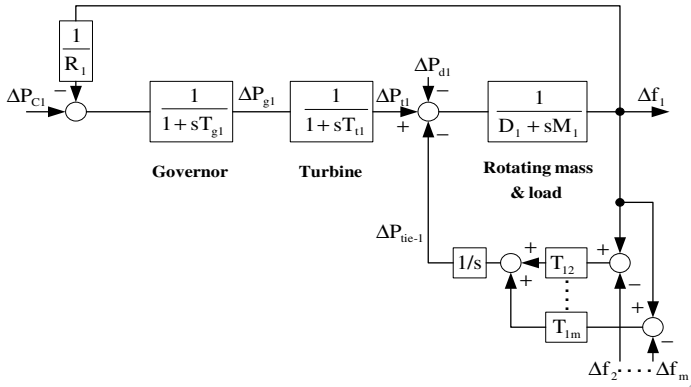

Fig. 1. Block diagram of control area-1.

ΔP_{ci} reference set point (control input) of area-i
ΔP_{ti} incremental output of generator in area-i
ΔP_{tie-i} incremental change in tie line power between area-i and other areas
ΔP_{di} disturbance in area-i
M_i equivalent inertia constant for area-i
D_i equivalent damping coefficient for area-i
T_{gi} governor time constant for area-i
T_{ti} turbine time constant for area-i
T_{ij} synchronizing coefficient in normal operating conditions between areas i and j
R_i drooping characteristic for area-i

The total real power imported to area-i equals the sum of all inflowing line powers P_{tie-ij} from adjoining areas, i.e.,

$$P_{tie-i} = \sum_j P_{tie-ij}. \tag{3}$$

The real power in per unit transmitted across a lossless line of reactance X_{ij} is

$$P_{tie-ij} = \frac{|V_i||V_j|}{X_{ij}P_{ri}} \sin(\delta_i - \delta_j) \tag{4}$$

where P_{ri} is the rated power of area-i, and

$$V_i = |V_i|e^{j\delta_i}, V_j = |V_j|e^{j\delta_j} \tag{5}$$

where $V_i = |V_i|e^{j\delta_i}$ and δ_i are the amplitude and the angle of the terminal voltage in area-i.

3. Synthesis procedure

3.1. Methodology

The main goal in each control area is maintaining the area frequency and tie line power interchanges close to specified values in the presence of model uncertainties and disturbances.

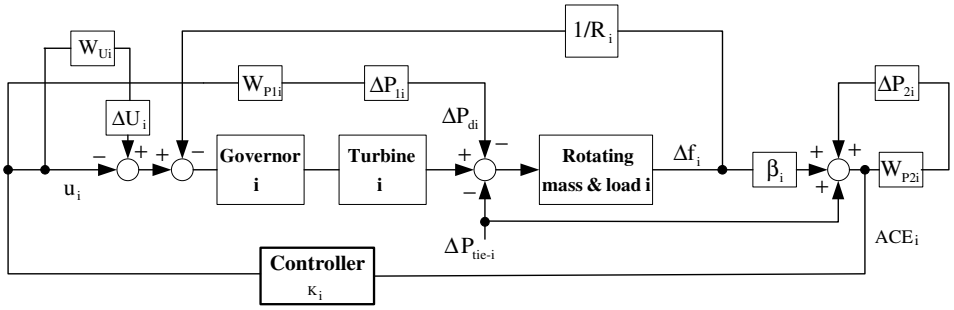

Fig. 2. Proposed strategy for load frequency controller synthesis in area-*i*.

To achieve our objectives and according to μ synthesis requirements, we can modify the control area model as shown in Fig. 2. In comparison with Fig. 1, the inter-area connections are removed, and it is considered by ΔP_{tie-i} that is properly weighted by inter-area connecting coefficients, and it is obtained from an integrator block. This figure shows the synthesis strategy for area-*i*.

It is notable that for each control area, there are several uncertainties because of parameter variations, model linearization and unmodeled dynamics due to approximation of the rest of the power system. Usually, the uncertainties in the power system can be modelled as multiplicative and/or additive uncertainties [14]. However, to keep the complexity of the controllers reasonably low, depending on the given control area, it is better to focus on the most important uncertainty. Sensitivity analysis of frequency stability due to parameters variation is a well known method for this purpose. In Fig. 2 the ΔU_i models the structured uncertainty set in the form of a multiplicative type and W_{U_i} includes the associated weighting function.

According to the requirements of performance and practical constraint on control actions, two fictitious uncertainties W_{P1i} and W_{P2i} are added to the control area model. The W_{P1i} on the control input sets a limit on the allowed control signal to penalize fast change and large overshoot in the control action. The weight W_{P2i} at the output sets the performance goal e.t. tracking/regulation error on the output deviation frequency. Furthermore, it is notable that in order to reject disturbances and to assure a good tracking property, W_{P1i} and W_{P2i} must be selected such that the singular value of sensitivity transfer function from u_i to y_i in related areas be reduced at low frequencies [15]. ΔU_i, Δp_{1i} and Δp_{2i} are uncertainty blocks associated with W_{Ui}, W_{P1i} and W_{P2i}, respectively.

The synthesis starts with setting the desired level of stability and performance for the first loop (control area) with a set of (u_i, y_i) and chosen uncertainties to achieve robust performance. In order to maintain adequate performance in the face of tie line power variation and load disturbances, the appropriate weighting functions must be used. The inclusion of uncertainties adequately allows for maximum flexibility in designing the control area closed loop characteristics, and the demands placed on the controller will increase. We can redraw Fig. 2 as shown in Fig. 3. g_{1i} and g_{2i} are transfer functions to the control output from the control input (u_i) and input disturbance (ΔP_{di}), respectively.

Fig. 4, shows the M–Δ configuration for area-*i*. G_{i-1} includes area-*i*'s nominal model and associated weighting functions and scaling factors. As is mentioned above, the blocks Δp_{1i} and Δp_{2i}

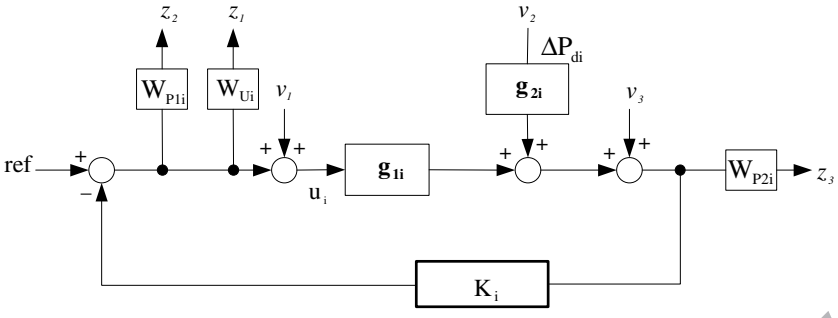

Fig. 3. Synthesis framework for area-*i*.

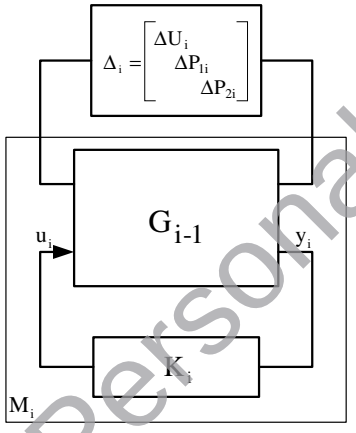

Fig. 4. M–Δ configuration for area-*i*.

are the fictitious uncertainties added to assure robust performance, while the block ΔU_i models the important multiplicative uncertainty associated with the control area model.

Now, in step i, the synthesis problem is designing the robust controller K_i. Based on the μ synthesis, the robust performance holds for a given M–Δ configuration (as shown in Fig. 4) if and only if

$$\inf_{K_i} \sup_{\omega \in R} \mu[M_i(j\omega)] < 1. \tag{6}$$

where, according to Fig. 3, M_i for the loop i (control area-i), is given by

$$M_i = \begin{bmatrix} -T_{0i}W_{Ui} & -g_{2i}g_{1i}^{-1}T_{0i}W_{Ui} & -g_{1i}^{-1}T_{0i}W_{Ui} \\ -T_{0i}W_{P1i} & -g_{2i}g_{1i}^{-1}T_{0i}W_{P1i} & -g_{1i}^{-1}T_{0i}W_{P1i} \\ g_{1i}S_{0i}W_{P2i} & g_{2i}S_{0i}W_{P2i} & S_{0i}W_{P2i} \end{bmatrix} \tag{7}$$

T_{0i} and S_{0i} are complementary sensitivity and sensitivity functions of the nominal model of control area-i and are given by

$$T_{0i} = g_{1i}K_i(1 + g_{1i}K_i)^{-1} \tag{8}$$

$$S_{0i} = 1 - T_{0i} = (1 + g_{1i}K_i)^{-1} \tag{9}$$

Using the performance robustness condition and the well known upper bound for μ, the robust synthesis problem, Eq. (6), reduces to determining

$$\min_{K_i} \inf_{D} \sup_{\omega} \overline{\sigma}(DM_i(j\omega)D^{-1}) \tag{10}$$

or equivalently

$$\min_{K_i,D} \left\| DM_i(G_{i-1}, K_i)(j\omega)D^{-1} \right\|_{\infty}, \tag{11}$$

by iteratively solving for D and K_i ($D-K$ iteration algorithm). Here, D is any positive definite symmetric matrix with appropriate dimension and $\overline{\sigma}(\cdot)$ denotes the maximum singular value of a matrix.

When the controller synthesis has been completed, another robust controller is designed for a second area with its set of variables and so on. During the design of each controller, the effects of previously designed controllers are being considered. The overall frame work of the proposed strategy is given in Fig. 5. It is notable that the block G_0 is assumed to contain the nominal open loop model, the appropriate weighting functions and scaling factors according to Δ_1. The block G_{m-1} includes G_0 and all decentralized controllers $K_1, K_2, \ldots, K_{m-1}$ designed in previous iterations $1, 2, \ldots, (m-1)$ and related uncertainty blocks.

We consider the nominal open loop state space representation of the power system as

$$\begin{aligned} \dot{x} &= Ax + Bu + Fd \\ y &= Cx \end{aligned} \tag{12}$$

where B corresponds to the control input, F corresponds to the disturbance inputs and C corresponds to the output measurement, which is input to the load frequency controller, and

$$\begin{aligned} x &= [\,\Delta f_1 \quad \Delta P_{t1} \quad \Delta P_{g1} \quad \Delta P_{tie-1} \cdots \Delta f_m \quad \Delta P_{tm} \quad \Delta P_{gm} \quad \Delta P_{tie-m}\,]^{\mathrm{T}} \\ u &= \Delta P_{c1} = u_1, \quad y = \beta \Delta f_1 + \Delta P_{tie-1} = y_1 \end{aligned} \tag{13}$$

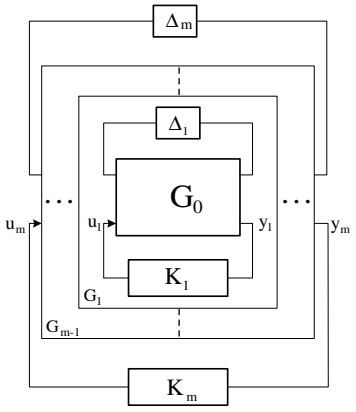

Fig. 5. Framework for μ synthesis.

It should be noted that the above equations for the open loop system, in each synthesis, must be augmented by including controllers synthesised in the previous steps. In each step, a μ controller is designed for one set of input and output variables. When this synthesis has been successfully completed, the next μ controller is designed for another set of input–output variables and so on. In every step, the effects of previously designed controllers are taken into account. Therefore, by adding one new loop at a time, the closed loop system remains stable at each step.

3.2. Synthesis steps

In summary, the proposed method consists of the following steps:

Step 1. Identify the order of loop synthesis.

The important problem with sequential design is that the final control performance achieved may depend on the order in which the controllers in the individual loops are synthesized. In order to overcome this problem, we must close the fast loops first because the loop gain and phase in the bandwidth region of the fast loops is relatively insensitive to the tuning of the lower loops. In other words, for those cases that the bandwidths of the loops are quite different, the outer loops are tuned with the inner (fast) loop in place. This causes a lower number of iterations during the re-tuning procedure to obtain the best possible performance [16].

Obtaining the estimation of the interactions on each control area behavior to determine the effects of undesigned loops is the other important issue in the sequential synthesis procedure. The determination of the performance relative gain array (PRGA) and the closed loop disturbance gain (CLDG) methods given in Ref. [17] are useful for this purpose.

Step 2. Identify the uncertainty blocks and associated weighting functions according to the first control area input–output set, depending on the dynamic model, practical limits and performance requirements.

It is notable that there is not any obligation to consider the uncertainty in only a few parameters. Considering the more complete model by including additional uncertainties is possible and causes less conservatism in the synthesis. However, the complexity of the computations and the order of result controller will increase.

Step 3. Isolate the uncertainties from the nominal area model, generate the Δp_{1i}, Δp_{2i}, ΔU_i blocks and perform the M–Δ feedback configuration (formulate the desired stability and performance).

Step 4. Start the D–K iteration using the μ synthesis toolbox to obtain the optimal controller, which provides desirable robust performance such that

$$\max_{\omega \in R} \mu[M(j\omega)] < 1 \tag{14}$$

ω denotes the frequency range for which the structured singular value is computed. This procedure determines the first robust controller.

Step 5. Reduce the order of result controller by utilizing the standard model reduction techniques and apply μ analysis to the closed loop system with reduced controller to check whether or not the upper bound of μ remains less than one.

It is notable that the controller found by this procedure is usually of a high order. In order to decrease the complexity of computation in the case of high order power systems, appropriate model reduction techniques might be applied both to the open loop system model and the $H\infty$ controller model within each D–K iteration.

Step 6. Continue this procedure by applying the above steps to other loops (control area input–output sets) according to the specified loop closing order in step 1.

Step 7. Retune the obtained controllers to achieve the best performance and check if the overall power system satisfies the robust performance condition using μ analysis.

If the objective is achievement of the best possible performance, the controller that was designed first must be removed and then re-designed, but now with controllers that have been synthesized in succeeding steps because the first synthesis was according to the more conservative state.

The proposed strategy in this paper guarantees the robust performance for multi-area power systems after design of the load frequency controllers according to the above sequential steps. The advantage of the procedure is it ensures that by closing one loop for a special area at a time, this area gets robust performance, and meanwhile, the multi-area power system holds its stability at each step. Similarly, during startup, the system will at least be stable if the loops are brought into service in the same order as they have been designed [17,18].

4. Applied to a four area power system

The controllers design approach presented in the previous section is now applied to a four areas power system shown in Fig. 6, and the nominal parameter values are assumed the same as Refs. [1,5,19] and are given in Table 1.

The nominal state space model for this system as a multi-input multi-output (MIMO) system can be constructed as Eq. (12) where

$$x = [\Delta f_1 \quad \Delta P_{t1} \quad \Delta P_{g1} \quad \Delta P_{tie-} \quad \Delta f_2 \quad \Delta P_{t2} \quad \Delta P_{g2} \quad \Delta P_{tie-2} \quad \Delta f_3 \quad \Delta P_{t3} \quad \Delta P_{g3} \quad \Delta P_{tie-3} \quad \Delta f_4 \quad \Delta P_{t4} \quad \Delta P_{g4} \quad \Delta P_{tie-4}]^{\mathrm{T}}$$
$$u = [u_1 \quad u_2 \quad u_3 \quad u_4]^{\mathrm{T}}, \quad d = [\Delta P_{d1} \quad \Delta P_{d2} \quad \Delta P_{d3} \quad \Delta P_{d4}]^{\mathrm{T}}, \quad y = [y_1 \quad y_2 \quad y_3 \quad y_4]^{\mathrm{T}}. \tag{15}$$

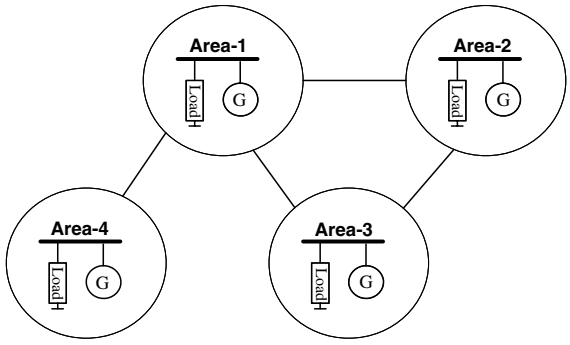

Fig. 6. Four area power system.

Table 1
Three area parameters

Parameter	Area-1	Area-2	Area-3	Area-4
D_i (pu Mw/Hz)	0.0083	0.0088	0.0080	0.0088
M_i (pu Mw)	0.166	0.222	0.16	0.13
T_{ti} (s)	0.3	0.33	0.35	0.375
T_{gi} (s)	0.08	0.072	0.07	0.085
R_i (Hz/pu Mw)	2.4	2.7	2.5	2.0
T_{ij} (pu Mw/Hz)	$T12 = T13 = T14 = T21 = T23 = T31 = T32 = T41 = 0.545$			

and $A \in R^{16\times16}$, $B \in R^{16\times4}$, $F \in R^{16\times4}$

$$A = \begin{bmatrix} A_{11} & A_{12} & A_{13} & A_{14} \\ A_{21} & A_{22} & A_{23} & A_{24} \\ A_{31} & A_{32} & A_{33} & A_{34} \\ A_{41} & A_{42} & A_{43} & A_{44} \end{bmatrix} \tag{16}$$

$$A_{ii} = \begin{bmatrix} -\frac{D_i}{M_i} & \frac{1}{M_i} & 0 & -\frac{1}{M_i} \\ 0 & -\frac{1}{T_{ti}} & \frac{1}{T_{ti}} & 0 \\ -\frac{1}{R_i T_{gi}} & 0 & -\frac{1}{T_{gi}} & 0 \\ \sum_j T_{ij} & 0 & 0 & 0 \end{bmatrix} \tag{17}$$

$$A_{ij}(i \neq j) = \begin{bmatrix} 0 & 0 & 0 & 0 \\ 0 & 0 & 0 & 0 \\ 0 & 0 & 0 & 0 \\ -T_{ij} & 0 & 0 & 0 \end{bmatrix} \tag{18}$$

and

$$B = \begin{bmatrix} 0 & 0 & \frac{-1}{T_{g1}} & 0 & 0 & 0 & 0 & 0 & 0 & 0 & 0 & 0 & 0 & 0 & 0 & 0 \\ 0 & 0 & 0 & 0 & 0 & 0 & \frac{-1}{T_{g2}} & 0 & 0 & 0 & 0 & 0 & 0 & 0 & 0 & 0 \\ 0 & 0 & 0 & 0 & 0 & 0 & 0 & 0 & 0 & 0 & \frac{-1}{T_{g3}} & 0 & 0 & 0 & 0 & 0 \\ 0 & 0 & 0 & 0 & 0 & 0 & 0 & 0 & 0 & 0 & 0 & 0 & 0 & 0 & \frac{-1}{T_{g4}} & 0 \end{bmatrix}$$

$$F = \begin{bmatrix} \frac{-1}{M_1} & 0 & 0 & 0 & 0 & 0 & 0 & 0 & 0 & 0 & 0 & 0 & 0 & 0 & 0 & 0 \\ 0 & 0 & 0 & 0 & \frac{-1}{M_2} & 0 & 0 & 0 & 0 & 0 & 0 & 0 & 0 & 0 & 0 & 0 \\ 0 & 0 & 0 & 0 & 0 & 0 & 0 & 0 & \frac{-1}{M_3} & 0 & 0 & 0 & 0 & 0 & 0 & 0 \\ 0 & 0 & 0 & 0 & 0 & 0 & 0 & 0 & 0 & 0 & 0 & 0 & \frac{-1}{M_4} & 0 & 0 & 0 \end{bmatrix}$$

The nominal open loop MIMO system is stable, including one oscillation mode. Simulation results show that the open loop system performance is affected by changes in the equivalent inertia constants M_i and synchronizing coefficients T_{ij}, more significantly than changes of other parameters within a reasonable range. Eigenvalue analysis shows that the considerable

Table 2
Instability conditions due to parameter variation

M_i	T_{ij}
$M_1 \leqslant 0.056$	$T_{12} \geqslant 0.645;\ T_{13} \geqslant 0.605$
$M_2 \leqslant 0.222$	$T_{14} \geqslant 0.605;\ T_{32} \geqslant 0.615$
$M_3 \leqslant 0.160$	$T_{21} \leqslant 0.475;\ T_{23} \leqslant 0.475$
$M_4 \leqslant 0.130$	$T_{31} \leqslant 0.445$

change in these parameters leads the power system to an unstable condition. Table 2 shows the variation range of each parameter, separately, that causes the open loop power system to be unstable.

Therefore, to demonstrate the capability of the proposed strategy for the problem at hand, in the viewpoint of uncertainty, our focus will be concentrated on variation of the M_i and T_{ij} parameters of all control areas, which are the important parameters from the control issue. Hence, for the given power system, we have set our objectives to area frequency regulation and assuring robust stability and performance in the presence of specified uncertainties and load disturbances as follows:

1. Holding stability and robust performance for the overall power system and each control area in the presence of 40% uncertainty for M_i and T_{ij}, which are assumed the sources of uncertainty associated with the given power system model.
2. Minimizing the effectiveness of step load disturbances (ΔP_{di}) on output signals.
3. Maintaining acceptable overshoot and settling time on the frequency deviation signal in each control area.
4. Set the reasonable limit on the control action signal in the change speed and amplitude viewpoint.

Following, we will discuss application of the proposed strategy on the given power system to meet the above objectives for each control area separately. Because of similarity and to save space, the first controller synthesis will be described in detail, and for the other control areas, only the final results will be presented. Since, for the problem at hand, the bandwidths of the four loops are not too different, the order of closing loops is not important. Therefore, we will start the synthesis procedure with control area 1.

4.1. Selection of weighting functions for the first control area loop

Uncertainty weight selection. As is mentioned in the previous section, we can consider the specified uncertainty in each area as a multiplicative uncertainty (W_{Ui}) associated with the nominal model. Corresponding to an uncertain parameter, let $\widehat{G}(s)$ denote the transfer function from the control input u_i to the control output y_i at operating points other than the nominal point. Following a practice common in robust control, we will represent this transfer function as

$$\widehat{G}(s) = G_0(s)(1 + \Delta_u(s)W_u(s)) \tag{19}$$

$\Delta_u(s)$ shows the uncertainty block corresponding to the uncertain parameter, $W_u(s)$ is the associated weighting function and $G_0(s)$ is the nominal transfer function model. Then, the multiplicative uncertainty block can be expressed as

$$|\Delta_u(s)W_u(s)| = \left|[\widehat{G}(s) - G_0(s)]G_0(s)^{-1}\right|, \quad G_0(s) \neq 0. \tag{20}$$

$W_u(s)$ is a fixed weighting function containing all the information available about the frequency distribution of the uncertainty, and where $\Delta_u(s)$ is a stable transfer function representing the model uncertainty. Furthermore, without loss of generality (by absorbing any scaling factor into $W_u(s)$ if necessary), it can be assumed that

$$\|\Delta_u(s)\|_\infty = \sup_\omega |\Delta_u(s)| \leqslant 1 \tag{21}$$

Thus, $W_u(s)$ is such that its respective magnitude Bode plot covers the Bode plot of all possible plants. Using Eq. (20), some sample uncertainties corresponding to different values of M_i and T_{ij} are obtained and shown in Fig. 7(a) and (b), respectively. It can be seen the frequency responses of both sets of parametric uncertainties are close to each other, and hence, to keep the complexity of the obtained controller low, we can model the uncertainties due to both sets of parameters variations by using a single, norm bonded multiplicative uncertainty to cover all possible plants as follows:

$$W_{U1}(s) = \frac{0.15(s^2 + 0.004)}{s^2 + 0.1s + 18}. \tag{22}$$

The frequency responses of $W_{U1}(s)$ are also shown in Fig. 7(b). This figure clearly shows that attempting to cover the uncertainties at all frequencies and finding a tighter fit using higher order transfer functions will result in an high order controller. The weight, Eq. (22), used in our design provides a conservative design at low and high frequencies, but it gives a good trade off between robustness and controller complexity.

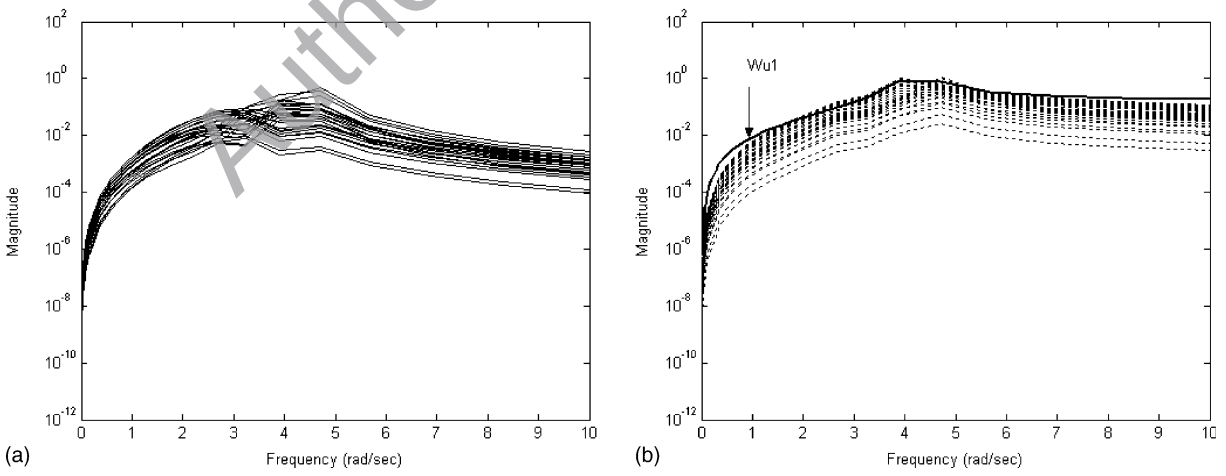

Fig. 7. Uncertainty plot due to change of: (a) M_i and (b) T_{ij} (dot) and $W_{U1}(s)$ (solid).

Performance weight selection. As we discussed in Section 3, in order to guarantee robust performance, we need to add to each control area a fictitious uncertainty block along with the corresponding performance weights W_{P11} and W_{P21} associated with the control area error minimization and control effort. In fact, an important issue in regard to selection of these weights is the degree to which they can guarantee the satisfaction of the design performance objectives.

Based on the following discussion, a suitable set of performance weighting functions that offer a good compromise among all the conflicting time domain specifications for control area-1, is

$$W_{P11}(s) = \frac{0.5s}{0.01s + 1}, \quad W_{P21}(s) = \frac{s + 0.75}{150s + 1}. \tag{23}$$

The selection of W_{P11} and W_{P21} entails a trade off among the different performance requirements. The weight on the control input W_{P11} was chosen close to a differentiator to penalize fast change and large overshoot in the control input. The weights on output error W_{P21} were chosen close to an integrator at low frequencies in order to get disturbance rejection, good tracking and zero steady state error. Additionally, as pointed out in the previous section, the order of the selected weights should be kept low in order to keep the controller complexity low.

Finally, we know that to reject disturbances and to track the command signal properly, it is required that the singular value of sensitivity function be reduced at low frequencies, and W_{P11} and W_{P21} must be selected such that this condition is satisfied. The interested reader can find suitable notes on choosing performance weighting functions in robust control techniques in Refs. [20–22].

Our next task is to isolate the uncertainties from the nominal plant model and redraw the system in the standard M–Δ configuration, which is shown in Fig. 8. By using the uncertainty description and developed performance weights, we get an uncertainty structure Δ with a scalar block (corresponding to the uncertainty) and a 2×2 block (corresponding to the performance). Having setup our robust synthesis problem in terms of the structured singular value theory, we use the μ analysis and synthesis toolbox [23], to obtain a solution.

The controller $K_1(s)$ is found at the end of three D–K iterations, yielding the value of about *0.893* on the upper bound on μ, thus guaranteeing robust performance. The resulting controller has a high order (21st). The controller is reduced to a fourth-order with no performance degra-

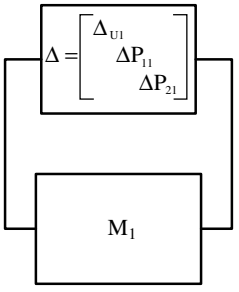

Fig. 8. Standard M–Δ block.

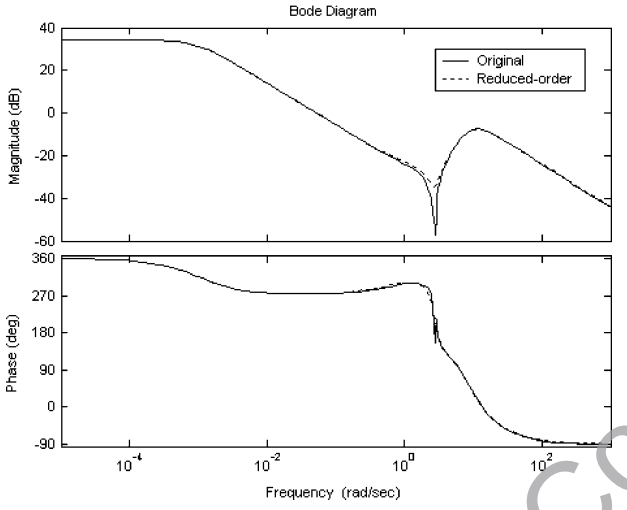

Fig. 9. Bode plots comparison of full order (original) and the reduced order controller $K_1(s)$.

dation ($\mu < 0.998$), using the standard Hankel Norm approximation. The Bode plots of the full-order controller and the reduced-order controller are shown in Fig. 9.

The transfer function of the reduced order controller is given as $K_1(s) = \frac{N_1(s)}{D_1(s)}$ with

$$\begin{aligned} N_1(s) &= 6.3905s^3 + 0.10604s^2 + 44.3998s + 37.994 \\ D_1(s) &= s^4 + 18.9617s^3 + 182.1594s^2 + 739.3578s + 0.7393 \end{aligned} \tag{24}$$

Using the same procedure and setting similar objectives as discussed above gives us the set of suitable weighting functions shown in Table 3, for the remaining loop synthesis. The order of the other obtained robust controllers without model reduction was 29(K_2), 37(K_3) and 45(K_4). These controllers can be approximated by lower order controllers as follows:

$$K_2(s) = \frac{N_2(s)}{D_2(s)}, \quad K_3(s) = \frac{N_3(s)}{D_3(s)}, \quad K_4(s) = \frac{N_4(s)}{D_4(s)} \tag{25}$$

Table 3
The set of weighting functions for control area loops 2, 3 and 4

Area-2	Area-3	Area-4
$W_{U2}(s) = \frac{0.1s^2 + 0.001}{s^2 + 0.2s + 21}$	$W_{U3}(s) = \frac{0.5s^2 + 0.005}{s^2 + 0.05s + 10}$	$W_{U4}(s) = \frac{0.11s^2 + 0.004}{s^2 + 0.11s + 15}$
$W_{p12}(s) = \frac{0.005s}{10^{-5}s + 4.5}$	$W_{p13}(s) = \frac{0.01s}{10^{-4}s + 1}$	$W_{p14}(s) = \frac{0.009s}{10^{-6}s + 15}$
$W_{p22}(s) = \frac{s + 0.1}{93(s + 0.001)}$	$W_{p23}(s) = \frac{s + 1.1}{100(s + 0.1)}$	$W_{p24}(s) = \frac{s + 0.22}{83(s + 0.02)}$

where

$$N_2(s) = 140.756s^5 + 164530.87s^4 + 194365.253s^3 + 98449.36s^2 + 546138.32s + 723970.37$$

$$D_2(s) = s^6 + 387.75s^5 + 35235.403s^4 + 67819.44s^3 + 2742801.2s^2 + 626558.42s + 126075.23$$

$$N_3(s) = 526.29s^5 + 1287.18s^4 - 1416.26s^3 + 6371.23s^2 + 12698.7s + 633.53$$

$$D_3(s) = s^6 + 7229.77s^5 + 6809.8s^4 + 93877.3s^3 + 101675.4s^2 + 4632.21s + 23.39$$

$$N_4(s) = 560.94s^6 + 8329.72s^5 + 4783.48s^4 + 1246.86s^3 + 19675.43s^2 + 2638.25s + 93.49$$

$$D_4(s) = s^7 + 18945.33s^6 + 12511.83s^5 + 76432.43s^4 + 836228.94s^3 + 42388.23s^2 + 1612.47s + 532$$

5. Simulation results

In order to demonstrate the effectiveness of the proposed method, some simulations were performed. In these simulations, the proposed scenario described in Section 3 was applied to the four area power system described in Section 4. In order to perform the simulation, the linear model of a nonreheating turbine in Fig. 1 is replaced by a nonlinear model of Fig. 10 (with ± 0.015 limits). This is to take into account the generating constraint (GRC), i.e. the practical constraint on the response speed of a turbine.

To test system performance, a step load disturbance of $\Delta P_{di} = 0.01\ pu$ is applied to each area, using the nominal plant parameters and those with uncertainty parameters by different percentage uncertainties. Since the system parameters for the four areas are identical and the ΔP_{tie} between two neighbor areas k and j is caused by $\Delta f_k - \Delta f_j$, the system performance can be mainly tested by applying the disturbance ΔP_{di} in the presence of the parameters uncertainties and observing the time response of Δf_i in each control area. Some selected time response simulation results are given in Figs. 11–14.

Fig. 11 shows the frequency deviation and control action signal in control areas 1 and 2, following the simultaneous step load disturbances of $\Delta P_{d1} = 0.01$ pu and $\Delta P_{d2} = 0.01$ pu. Fig. 12, shows the frequency deviation following a step load disturbance of $\Delta P_{d1} = 0.01$ pu, $\Delta P_{d2} = 0.01$ pu and a 40% increase of M_i and T_{ij} in all areas, simultaneously.

Fig. 13 shows the similar simulation result for control areas 3 and 4 ($\Delta P_{d3} = 0.01\ pu$, $\Delta P_{d4} = 0.01\ pu$ and a 40% increase in M_i and T_{ij} in all areas). Fig. 13(b) shows the control signals

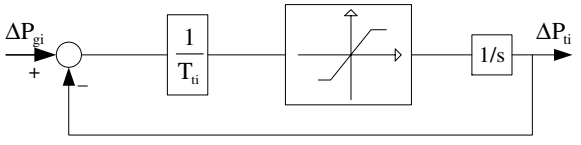

Fig. 10. The GRC constraint in the nonlinear turbine model.

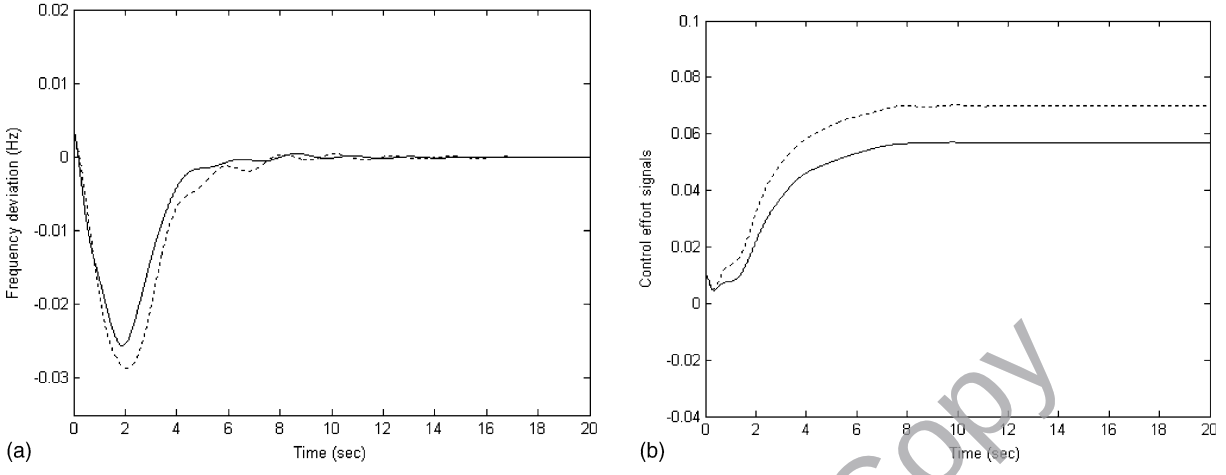

Fig. 11. (a) Frequency deviation; (b) control signals, in areas 1 (solid) and 2 (dot), following a 0.01 pu step load disturbance in both areas.

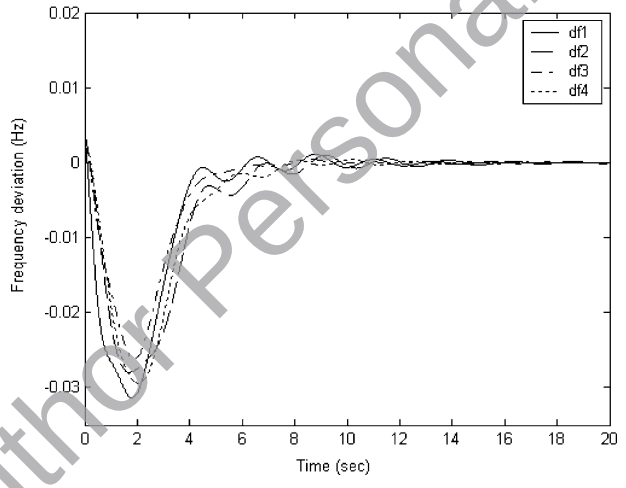

Fig. 12. Frequency deviation in presence of $\Delta P_{d3} = \Delta P_{d4} = 0.01$ pu and 40% increase M_i and T_{ij}.

corresponding to control areas 3 and 4. Finally, Fig. 14 shows the power system response for the assigned possible worst case, i.e. a step load disturbance in each area and a 40% decrease in the uncertain parameters, simultaneously.

These simulation results demonstrate the effectiveness of the proposed strategy in order to provide robust frequency regulation in multi-area power systems. Although, because of our tight design objectives with considering several simultaneous uncertainties and input disturbances, the orders of the resulting robust load frequency controllers were relatively high (in comparison with classical or some new methods, such as Refs. [5,19]), the proposed method gives better performance in the view point of disturbance rejection and frequency error minimization in the presence of model uncertainties.

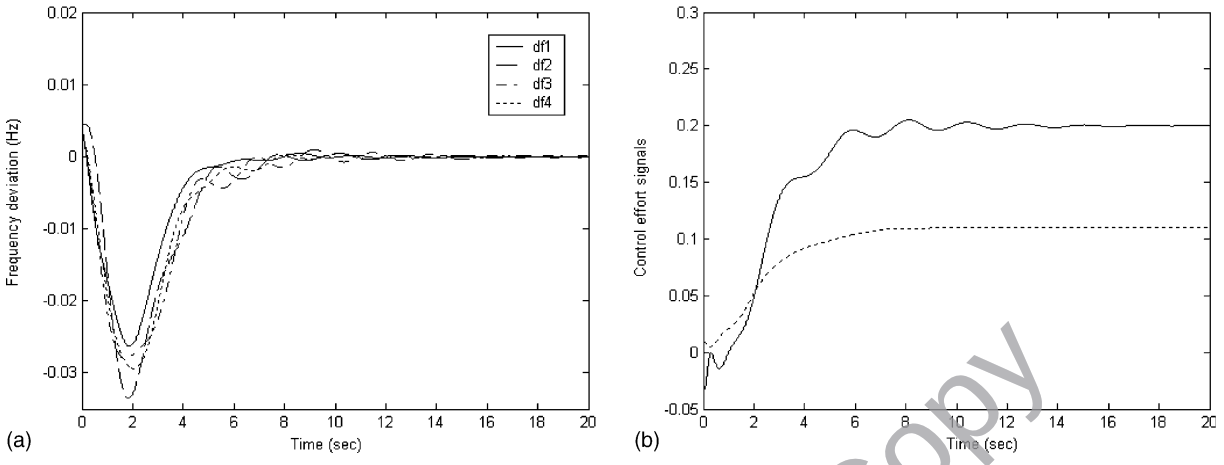

Fig. 13. (a) Frequency deviation; (b) u_3 and u_4, in presence of $\Delta P_{d3} = \Delta P_{d4} = 0.01$ pu and +40% change in uncertain parameters.

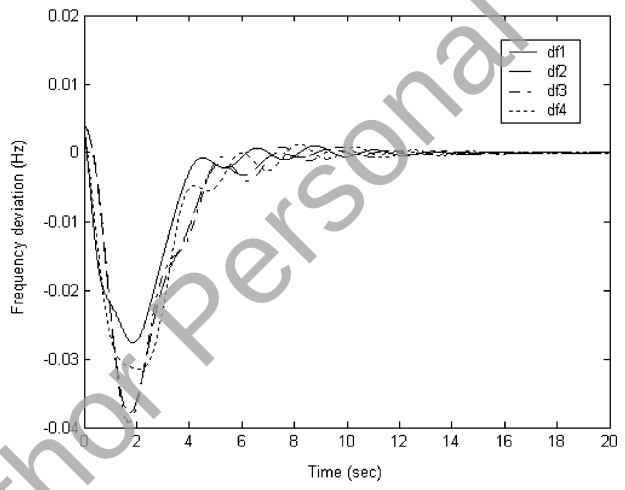

Fig. 14. Frequency deviation following a step load disturbance $\Delta P_{di} = 0.01$ pu in each area and −40% change in uncertain parameters.

6. Conclusion

In this paper, a new systematic method for robust sequential decentralized load frequency controllers using μ synthesis in an interconnected multi-area power system has been proposed. At each design step, the information about the controllers designed in the previous step are taken into account. Therefore, the method can be less conservative than independent decentralized design and more practical than proposed simultaneous decentralized load frequency controllers.

The design strategy includes enough flexibility to set the desired level of stability and performance and consider the practical constraints by introducing appropriate uncertainties. The simulation results demonstrate the effectiveness of the proposed method for solution the LFC problem in the presence of uncertainties and load disturbances in multi-area power systems.

Acknowledgements

The authors are grateful to Prof. T. Hiyama from Kumamoto University and Dr. G. Fujita from Shibaura Institute of Technology for their kind discussions.

References

[1] Hiyama T. Design of decentralised load–frequency regulators for interconnected power systems. IEE Proc C 1982;129:17–23.
[2] Feliachi A. Optimal decentralized load frequency control. IEEE Trans Power Syst 1987;PWRS-2:379–84.
[3] Liaw CM, Chao KH. On the design of an optimal automatic generation controller for interconnected power systems. Int J Contr 1993;58:113–27.
[4] Ishi T, Shirai G, Fujita G. Decentralized load frequency based on H-inf control. Electr Eng Jpn 2001;136(3):28–38.
[5] Yang TC, Cimen H, Zhu QM. Decentralised load frequency controller design based on structured singular values. IEE Proc Gener Transm Distrib 1998;145(1):7–14.
[6] Kazemi MH, Karrari M, Menhaj MB. Decentralized robust adaptive-output feedback controller for power system load frequency control. Electr Eng J 2002;84:75–83.
[7] Kia YL, Youyi W, Zhou R. Decentralized robust load–frequency control in coordination with frequency-controllable HVDC links. Electr Power Energy Syst 1997;19(7):423–31.
[8] Rerkpreedapong D, Feliachi A. Decentralized load frequency control for load following services. In: IEEE-PES Winter Meeting, vol. 2; 2000. pp. 1252–7.
[9] El-Sherbiny MK, El-Saady G, Yousef AM. Efficient fuzzy logic load frequency controller. Energy Conver Manage 2002;43:1853–63.
[10] Bevrani H. Application of Kharitonov's theorem and its results in load–frequency control design. J Electr Sci Technol—BARGH 1998;24:82–95.
[11] Chiu M, Arkun Y. A methodology for sequential design of robust decentralized control systems. Automatica 1992;28:997–1001.
[12] Doyel JC. Analysis of feedback systems with structured uncertainties. IEE Proc D 1982;129:242–50.
[13] Bevrani H, Mitani Y, Tsuji K. Sequential decentralized design of load frequency controllers in multiarea power systems. In: IFAC Symposium on Power Plants and Power Systems Control 2003, Seoul Korea [accepted for presentation].
[14] Djukanovic M, Khammash M, Vittal V. Structured singular value theory based stability robustness of power systems. Proc IEEE CDC 1997:2702–7.
[15] Bevrani H. Robust load frequency controller in a deregulated environment: a μ synthesis approach. In: Proceedings of IEEE International Conference on Control Applications; 1999. p. 616–21.
[16] Skogestad S, Postlethwaite I. Multivariable feedback control. New York: John Wiley & Sons; 2000. p. 397–448.
[17] Hovd M, Skogestad S. Sequential design of decentralised controllers. Automatica 1994;30:1607–10.
[18] Djukanovic M, Khammash M, Vittal V. Sequential synthesis of structured singular value based decentralised controllers in power systems. IEEE Trans Power Syst 1999;14:635–41.
[19] Yang TC, Ding ZT, Yu H. Decentralised power system load frequency control beyond the limit of diagonal dominance. Electr Power Energy Syst 2002;24:173–84.
[20] Zhou K, Doyel JC. Essentials of robust control. Englewood Cliffs, NJ: Prentice-Hall; 1998. p. 88–94.
[21] Lundstrom P, Skogestad S, Wang ZQ. Performance weight selection for H-inf and μ-control Method. Trans Inst Meas Contr 1991;13(5):241–52.
[22] Bevrani H, Mitani Y, Tsuji K. Robust load frequency regulation in a new distributed generation environment. In: 2003 IEEE-PES General Meeting, Toronto, Canada [accepted for presentation].
[23] Balas GJ, Doyle JC, Glover K, Packard A, Smith R. μ-Analysis and synthesis toolbox for use with MATLAB. The MathWorks Inc; 1995.